

Permeability Effects on Irregular Wave Runup and Reflection

Nobuhisa Kobayashi, Daniel T. Cox and Andojo Wurjanto

Center for Applied Coastal Research
Department of Civil Engineering
University of Delaware
Newark, DE 19716, USA



ABSTRACT

KOBAYASHI, N., COX, D.T., and WURJANTO, A., 1990. Permeability effects on irregular wave runup and reflection. *Journal of Coastal Research*, 7(1), 127-136. Fort Lauderdale (Florida), ISSN 0749-0208.

Six small-scale test runs were conducted to examine the detailed spectral and time series characteristics of irregular wave reflection and runup on 1:3 rough impermeable and permeable slopes. The permeability effects reduced the average reflection coefficient and significant runup as was observed by a number of researchers. The permeability effects on irregular wave reflection were found to reduce the reflection coefficient fairly uniformly over the wind wave frequency range. The permeability effects on irregular wave runup were found to reduce the low frequency wave components significantly. The measured runup distributions in the range of the exceedance probability greater than approximately 0.02 were represented by the Rayleigh distribution fairly well.

ADDITIONAL INDEX WORDS: *Irregular wave, runup, reflection, permeability, breakwaters, experiment.*

INTRODUCTION

Irregular wave runup and reflection are important for the design of a coastal structure against wind waves. Extensive data on regular wave runup and reflection are available, but published data on irregular wave runup and reflection are fairly limited (*e.g.*, BRUUN, 1985). The limited irregular wave runup data suggested that the irregular wave runup distribution might be approximated by the Rayleigh distribution (*e.g.*, BATTJES, 1971; LOSADA and GIMENEZ-CURTO, 1981). The data of AHRENS (1983) on irregular wave runup on plane, smooth slopes ranging from 1 on 1 to 1 on 4 indicated the importance of wave setup and runup interaction on the smooth slopes for breaking waves. For gentler smooth slopes, low frequency shoreline oscillations may become dominant in view of available data on swash oscillations on natural beaches (*e.g.*, GUZA and THORNTON, 1982; HOLMAN and SALLENGER, 1985). As for irregular wave reflection, SEELIG (1983) proposed empirical formulas in which the average reflection coefficient was expressed as a function of the surf

similarity parameter. However, the average reflection coefficient may not be sufficient for irregular waves since the irregular wave reflection and dissipation should depend on the frequency of random waves as observed on natural beaches (*e.g.*, TATAVARTI *et al.*, 1988).

In order to obtain detailed data on irregular wave reflection and runup on rough permeable and impermeable slopes, six test runs were conducted in a wave tank. Three different incident irregular wave trains representing dominant breaker types of plunging, collapsing and surging waves were generated by a piston-type wave paddle following a fairly standard method for random wave generation (*e.g.*, GODA, 1985). Rough impermeable and permeable slopes were exposed to the three different incident waves to examine the effects of permeability on irregular wave runup and reflection. The rough impermeable slope consisted of a 1:3 glued gravel slope with an impermeable base, whereas the rough permeable slope was constructed by placing a thick layer of gravel on top of the 1:3 glued gravel slope. For each of the six runs, measurements were made of the incident and reflected waves in front of the slope and the waterline oscillations on the slope. The spectral and time

series characteristics of the measured temporal variations are analyzed herein to examine the hydrodynamic processes involved in the irregular wave reflection and runup on the rough permeable and impermeable slopes.

EXPERIMENT

The irregular wave tests summarized herein were described in detail by COX (1989). The wave tank was 30 m long, 2.5 m wide and 1.5 m high. The water depth in the tank was 0.4 m as shown in Figure 1. Irregular wave trains were generated with a piston-type wave paddle driven by a hydraulic actuator and controlled by a computer. A 1:3 plywood slope supported by a steel frame was installed at the opposite end of the tank. The distance between the wave paddle and the toe of the 1:3 plywood slope was 25 m. A single layer of gravel was glued on the plywood base to produce a 1:3 rough impermeable slope. The corresponding permeable slope was constructed by placing a thick layer of the same gravel on top of the 1:3 rough impermeable slope. The thickness of the permeable gravel layer normal to the plywood base was 0.2 m as indicated in Figure 1 for the permeable slope.

The gravel used in the experiment was well-sorted crushed granite. The median diameter of the gravel units based on a standard sieve analysis was 2.1 cm. The measurement of the dry and submerged weight of 50 gravel units indicated that the median gravel mass was 14.8 g and the specific density was 2.7, where fresh-water of temperature 20°C was used in the experiment. The angle of repose of the gravel

was approximately 50°. The porosity of the permeable gravel layer was 0.48 based on the measurement of the volume and weight of a sample of gravel units including void and the weight of the sample filled with water. For the permeable slope tests, loose gravel units were exposed to wave action and allowed to settle before the actual tests to minimize the slope profile change during the tests. Loose gravel units placed on the permeable slope were observed to remain at their initial locations without being dislodged during the tests. It should be noted that loose gravel units placed on the glued gravel slope were dislodged during the impermeable slope tests. As a result, the permeability of the thick gravel layer increased the stability of loose gravel units noticeably. This is consistent with the findings of VAN DER MEER (1988).

Three wire resistance wave gages placed along the centerline of the tank were used to measure the free surface oscillations at $x = 0$, -0.3 and -0.9 m seaward of the toe of the 1:3 permeable or impermeable slope, where the horizontal coordinate x is taken to be a positive landward with $x = 0$ at the toe of the slope. It should be noted that the location $x = 0$ for the permeable slope was 0.63 m seaward of that for the impermeable slope because of the presence of the 0.2 m thick gravel layer. Each gage consisted of two platinum wires stretched between an aluminum frame connected to a movable staff. The gages were calibrated separately using stepper motors controlled by a computer which raised or lowered the wave staffs. The calibration error was ± 5 mm or less. The incident and reflected wave trains were separated

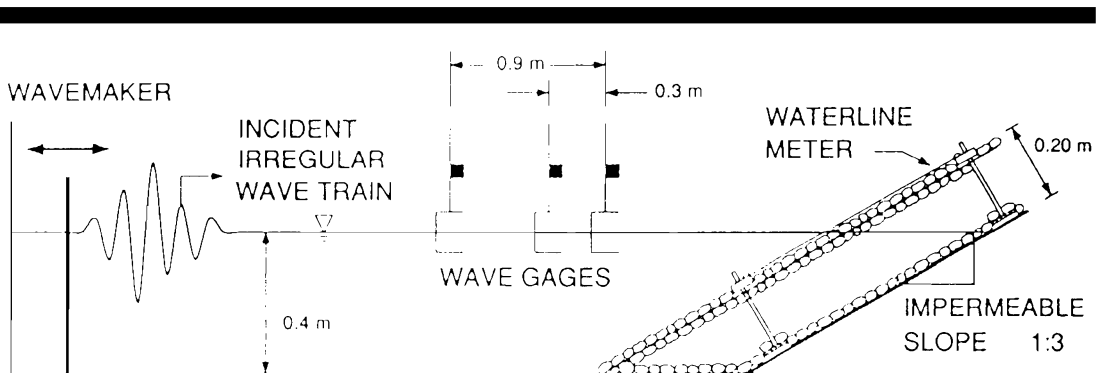


Figure 1. Schematic of experimental setup for permeable slope tests.

using the method of SEELIG (1980). The effective range of resolution was taken as $0.05 < (\Delta x/L) < 0.45$ on the basis of the guideline of GODA (1985), where the spacing of two gages, Δx , was 0.3, 0.6 and 0.9 m for these tests and the wavelength, L , was estimated using linear wave theory. Correspondingly, the effective frequency range of resolution was $0.11 \text{ Hz} < f < 1.5 \text{ Hz}$. The incident wave spectra specified for controlling the wave paddle motion were chosen such that the wave energy outside the effective frequency range could be neglected.

A wire resistance gage similar to the wave gages was used to measure the waterline oscillation along the centerline of the 1:3 permeable and impermeable slopes. The gage consisted of two platinum wires attached to Plexiglas plates which were fixed to threaded stainless steel rods. The steel rods were bolted to the plywood slope for the impermeable slope tests and supported by the steel plates placed on the glued gravel slope for the permeable slope tests as shown in Figure 1. The average vertical distance of the wires above the irregular surface of the permeable or impermeable slope was approximately 1 cm. For calibration, use was made of a second gage, which consisted of wires mounted on a Plexiglas staff with dimensions similar to the fixed gage. The staff was free to move along the Plexiglas track which was mounted parallel to the fixed gage. The movable gage was calibrated manually by sliding the staff into the water. A side-by-side comparison of the two gages made by raising and lowering the water level in the tank indicated that the calibration curves of the two gages were within the calibration error.

Three different irregular wave trains representing dominant breaker types of plunging, collapsing and surging waves on the 1:3 slope were generated by the wave paddle on the basis of the TMA spectrum in finite water depth proposed by BOUWS *et al.* (1985) together with random phases. The wave heights were selected to be small relative to the water depth since the standard method for simulating random wave trains may not reproduce wave group statistics in very shallow water (ELGAR *et al.*, 1984). The required motion of the wave paddle was calculated without regard to free second-harmonic waves (MADSEN, 1971), spurious low frequency waves (BARTHEL *et al.*, 1983), wave transformation in the tank, and wave reflection

from the paddle. Ideally speaking, incident wind waves and group bounded long waves (LONGUET-HIGGINS and STEWART, 1962) should have been reproduced without spurious waves caused by the paddle motion and with active absorption at the paddle of waves reflected from the slope (MILGRAM, 1970; KOSTENSE, 1984). In order to compensate the limitations of the wave generation, the measured incident and reflected waves for each test were used in the following data analyses.

Three test runs were conducted for the 1:3 rough impermeable slope and denoted by runs I1, I2 and I3 for which observed dominant breaker types were plunging, collapsing and surging waves, respectively. The three tests were repeated for the 1:3 rough permeable slope and denoted by runs P1, P2 and P3. The specified motion of the wave paddle controlled by a computer was the same for runs IJ and PJ with $J = 1, 2$ and 3 . For each run, the measurements of the free surface oscillations at the three locations and the waterline oscillation on the 1:3 permeable or impermeable slope were synchronized. The sampling rate for each temporal measurement was taken to be 32 Hz for runs I1 and P1, 20 Hz for runs I2 and P2, and 16 Hz for runs I3 and P3. This sampling rate corresponded to about 30 data points per mean wave period. The duration of the measurements used for the subsequent time series and spectral analyses was 185 sec for runs I1 and P1 and 365 sec for runs I2, I3, P2 and P3. This duration corresponded to about 200 individual waves in the incident wave train. The measured waterline oscillation for each run was expressed in terms of its elevation Z_r above the still water level (SWL) as a function of time t .

In order to estimate the incident and reflected wave trains for each run, the measured time series of the free surface oscillation η at $x = 0, -0.3$ and -0.9 m were analyzed using a Fast Fourier transform. The time-averaged values of η were essentially zero. The computed Fourier coefficients outside the effective frequency range $0.11 \text{ Hz} < f < 1.5 \text{ Hz}$ were negligible. This indicated that seiching motions in the frequency range $f < 0.11 \text{ Hz}$ were negligible in the wave tank. The Fourier coefficients associated with the incident wave train $\eta_i(t,x)$ and the reflected wave train $\eta_r(t,x)$ in the region $-0.9 \text{ m} \leq x \leq 0.0 \text{ m}$ were calculated from the Fourier coefficients of the measured time series $\eta(t,x)$

assuming that $\eta(t,x) = [\eta_i(t,x) + \eta_r(t,x)]$ at $x = 0.0, -0.3$ and -0.9 m. Use was made of the average values of the calculated Fourier coefficients for each pair of the three measurements within the effective frequency range of resolution (SEELIG, 1980; GODA, 1985). An inverse Fast Fourier transform was then used to compute the time series $\eta_i(t,x)$ and $\eta_r(t,x)$ at $x = 0$, which are called the incident wave train $\eta_i(t)$ and the reflected wave train $\eta_r(t)$ at the toe of the slope in the following. The incident wave spectrum corresponding to the incident wave train $\eta_i(t)$ was found to be fairly similar to the TMA spectrum specified for the motion of the wave paddle.

INCIDENT AND REFLECTED IRREGULAR WAVES

The incident wave train $\eta_i(t)$ at the toe of the slope for each run was analyzed using a zero upcrossing method. Table 1 shows the values of the significant wave height H_s and the mean period T_m of the zero upcrossings for each run. Comparing the values of H_s and T_m for the corresponding impermeable and permeable test runs, the values of T_m are almost the same but the value of H_s for the permeable test run is slightly less than that for the impermeable test run. This is probably because of the wave reflection from the slope which was reduced by the presence of the thick gravel layer, while the waves reflected from the slope were re-reflected by the wave paddle. As a result, the identical paddle motion did not result in exactly the same incident wave trains for the permeable and impermeable test runs. In order to account for the small differences of the wave heights and periods, the measured time series are normalized by H_s and T_m in the following, although

other wave heights and periods could also be used for the normalization.

Table 1 lists the values of H_{rms}/H_s , T_s/T_m and ξ for each run, where H_{rms} is the root-mean-square wave height, T_s is the significant wave height, and ξ is the surf similarity parameter based on H_s and T_m . The spectral density of the incident wave train $\eta_i(t)$ was also computed for each run. Table 1 lists the values of H_{m0}/H_s , T_p/T_m and ξ_p , where H_{m0} is the spectral estimate of the significant wave height given by $H_{m0} = 4\sqrt{m_0}$ with m_0 being the zeroth moment of the incident wave spectrum, T_p is the spectral peak period, and ξ_p is the surf similarity parameter based on H_{m0} and T_p . In short, the time series and spectral characteristics of the incident wave trains for the corresponding impermeable and permeable slope tests were almost the same except that the wave heights such as H_s , H_{rms} and H_{m0} were reduced slightly by the presence of the thick gravel layer.

The incident wave spectra S_i normalized by $T_m H_s^2$ for the six test runs are plotted as a function of the normalized frequency, $f_* = f T_m$, in Figure 2. The spectra shown in this paper are the smoothed spectra with 16 degrees of freedom (e.g., GODA, 1985). The normalized frequency range of resolution of the incident and reflected waves for these tests is $0.12 < f_* < 1.6$ for runs I1 and P1, $0.15 < f_* < 2.0$ for runs I2 and P2, and $0.19 < f_* < 2.6$ for runs I3 and P3. The normalized spectra $S_i(f_*)$ for the corresponding impermeable and permeable slope test runs agree well except for the low frequency range where the normalized frequency f_* is less than about 0.5. The incident low frequency wave components were not reproduced in the present experiment. Figure 2 indicates that the thick gravel layer reduces the incident low frequency wave components in the tank. This finding appears to be consistent with the

Table 1. Time series and spectral parameters of incident irregular waves for six test runs.

| Run No. | H_s (cm) | T_m (sec) | H_{rms} | T_s | ξ | H_{m0} | T_p | ξ_p |
|---------|------------|-------------|-----------|-------|-------|----------|-------|---------|
| | | | H_s | T_m | | H_s | T_m | |
| I1 | 7.05 | 1.07 | 0.71 | 1.02 | 1.68 | 1.02 | 1.15 | 1.91 |
| I2 | 5.61 | 1.36 | 0.70 | 1.19 | 2.39 | 1.04 | 1.41 | 3.30 |
| I3 | 5.08 | 1.71 | 0.70 | 1.30 | 3.15 | 1.06 | 1.62 | 4.96 |
| P1 | 6.85 | 1.08 | 0.71 | 1.01 | 1.72 | 1.01 | 1.04 | 1.78 |
| P2 | 5.35 | 1.36 | 0.71 | 1.17 | 2.44 | 1.04 | 1.56 | 3.73 |
| P3 | 4.57 | 1.74 | 0.71 | 1.25 | 3.39 | 1.06 | 1.58 | 5.20 |

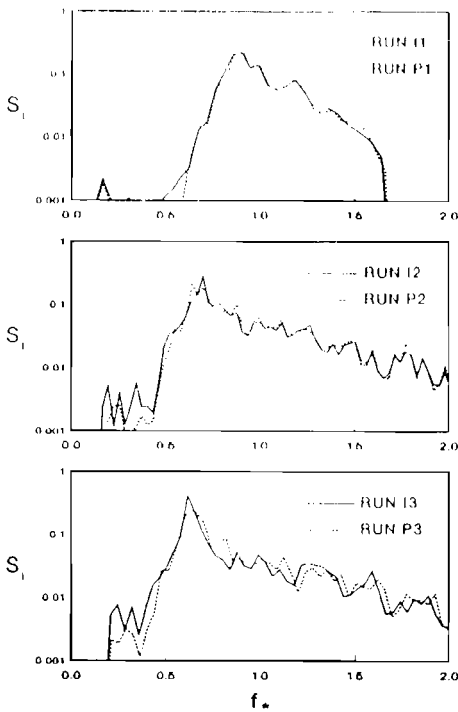


Figure 2. Normalized incident wave spectra for six test runs.

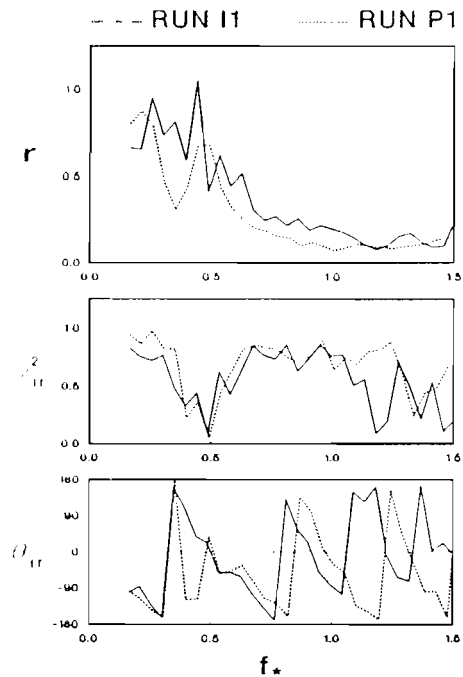


Figure 3. Reflection coefficient, coherence and phase for reflected waves for runs I1 and P1.

experiment of MANSARD and BARTHEL (1984) in which a gravel beach was used to absorb the incident wind waves and group bounded long waves.

The spectral density S_r of the reflected wave train at the toe of the slope was computed and normalized by $T_m H_s^2$ for each run. In order to examine the frequency dependence of wave reflection, the reflection coefficient r for given normalized frequency f_* defined as $r = [S_r(f_*)/S_i(f_*)]^2$ is plotted in Figures 3, 4 and 5 for each pair of the impermeable and permeable slope tests. The average reflection coefficient \bar{r} may be defined as $\bar{r} = [(m_o)_r/m_o]^2$ where $(m_o)_r$ and m_o are the zeroth moments of $S_r(f_*)$ and $S_i(f_*)$, respectively. The value of \bar{r} for each test run is listed in Table 2. The decrease of \bar{r} with the decrease of ξ and ξ_p and due to the presence of the thick gravel layer is consistent with the empirical results of SEELIG (1983). Figures 3, 4 and 5 indicate that the wave reflection from the impermeable and permeable slopes tends to decrease with the increase of the frequency of wave components. Moreover, the permeability

effects tend to reduce the reflection coefficient r uniformly over the wind wave frequency range where the normalized frequency f_* is greater than about 0.5.

Figures 3, 4 and 5 also show the coherence squared, γ_{ir}^2 , and the phase difference, θ_{ir} , in degrees of the cross spectrum between the incident and reflected wave trains at the toe of the slope located at $x = 0$ for each pair of the test runs. The low coherence for runs I1 and P1 may have been caused partly by the errors of the measurement of the relatively small reflected wave trains. The decrease of the coherence from unity with increasing frequency appears to be similar to that observed by THORNTON and CALHOUN (1972) and may be caused partly by the scattering of wave components with shorter periods by the gravel units. The permeability effects on the coherence are essentially limited to this high frequency range. The phase difference θ_{ir} between the incident and reflected waves at the toe of the slope is plotted in the range of -180° to 180° in Figures 3, 4 and 5. For the frequency range of the high coherence, the

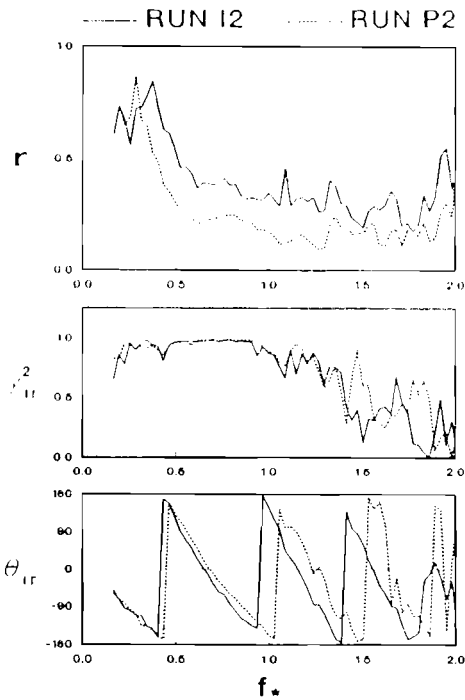


Figure 4. Reflection coefficient, coherence and phase for reflected waves for runs I2 and P2.

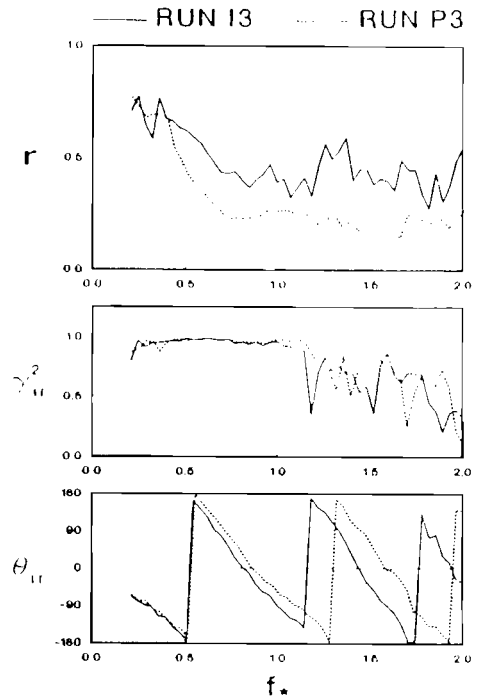


Figure 5. Reflection coefficient, coherence and phase for reflected waves for runs I3 and P3.

normalized travel time for the wave component with given f_* propagating upslope from $x = 0$ and then downslope to $x = 0$ may be estimated as $-\theta_{ir}/(2\pi f_*)$ in which θ_{ir} should decrease monotonically with increasing frequency without the restriction of $-180^\circ \leq \theta_{ir} \leq 180^\circ$. Figures 3, 4 and 5 suggest that the normalized travel time on the impermeable slope is slightly greater than that on the corresponding permeable slope. The normalized travel time may be affected by wave runup which is larger on the impermeable slope than on the corresponding permeable slope. Wave reflection from the permeable slope seems to occur at the surface of the gravel layer rather than at the impermeable plywood base which was located 0.63 m horizontally landward. This is because the increase of the horizontal distance should have resulted in the increase of the normalized travel time. However, it should be stated that the interpretations of the measured cross spectra on the basis of linear wave theory are only qualitative since the wave motion on the 1:3 slope is highly nonlinear.

IRREGULAR WAVE RUNUP

The measured waterline oscillation on the slope expressed in terms of its elevation Z_r above SWL as a function of time t is averaged over the duration of its measurement to obtain the time-averaged value denoted by \bar{Z}_r , which is wave setup on the slope. The measured values of \bar{Z}_r/H_s for the six test runs listed in Table 2 indicate a significant reduction of wave setup on the permeable slope. Wave setup on the slope

Table 2. Average wave reflection coefficient \bar{r} , wave setup \bar{Z}_r , significant swash height h_s , significant runup R_s , and maximum runup R_{max} for six test runs.

| Run No. | ξ | \bar{r} | \bar{Z}_r | h_s | R_s | R_{max} |
|---------|-------|-----------|-------------|-------|-------|-----------|
| | | | H_s | H_s | H_s | H_s |
| I1 | 1.68 | 0.21 | 0.13 | 1.16 | 0.79 | 1.67 |
| I2 | 2.39 | 0.37 | 0.17 | 2.19 | 1.34 | 2.52 |
| I3 | 3.15 | 0.48 | 0.20 | 3.19 | 1.90 | 3.10 |
| P1 | 1.72 | 0.13 | 0.05 | 1.05 | 0.67 | 1.32 |
| P2 | 2.44 | 0.22 | 0.05 | 1.58 | 0.96 | 1.46 |
| P3 | 3.39 | 0.28 | 0.05 | 2.09 | 1.19 | 2.28 |

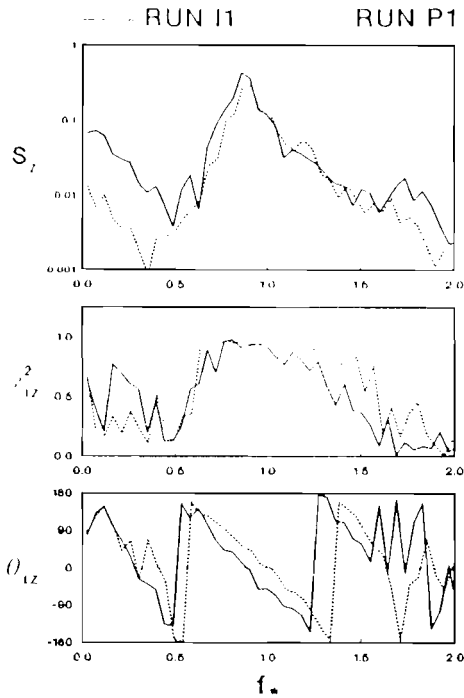


Figure 6. Spectrum, coherence and phase of waterline oscillations for runs I1 and P1.

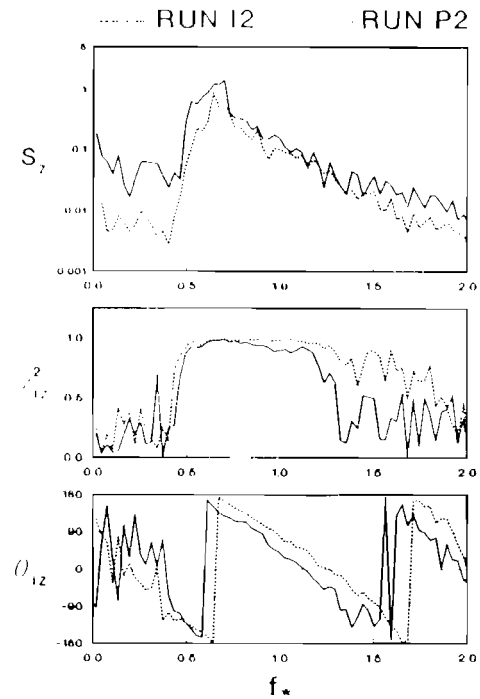


Figure 7. Spectrum, coherence and phase of waterline oscillations for runs I2 and P2.

is expected to be related to the increase of the mean water level inside the permeable layer, which was not measured in the present experiment. BRUUN and JOHANNESSON (1976) made such measurements and found that the mean water level in porous breakwaters increased more as the permeability was reduced. As a result, the present experimental results are consistent with their results.

The spectral density of the time series $[Z_r(t) - \bar{Z}_r]$ was computed and normalized by $T_m H_s^2$ for each run. The normalized spectrum of the waterline oscillation is denoted by S_z as a function of the normalized frequency, $f_* = fT_m$. The spectra $S_z(f_*)$ for the corresponding impermeable and permeable slope test runs are plotted in Figures 6, 7 and 8. The spectra shown in these figures are the smoothed spectra with 16 degrees of freedom. It is noted that the frequency range of resolution imposed on $S_z(f_*)$ and $S_i(f_*)$ is not required for $S_z(f_*)$. These figures show noticeable low frequency wave components in the waterline oscillation on the 1:3 rough impermeable slope. These low frequency

wave components are small relative to the wave components in the incident wind wave frequency band, unlike swash oscillations on natural beaches (GUZA and THORNTON, 1982; HOLMAN and SALLENGER, 1985). The low frequency wave components are reduced significantly for the permeable slope test runs. On the other hand, the high frequency wave components are affected little by the presence of the thick gravel layer.

Figures 6, 7 and 8 also show the coherence squared, γ_{12}^2 , and the phase difference, θ_{12} , in degrees of the cross spectrum between the incident wave train and the waterline oscillation on the slope for each pair of the test runs. The coherence is almost unity in the vicinity of the peak of the spectrum $S_z(f_*)$ which is located approximately at the peak of the corresponding incident wave spectrum $S_i(f_*)$ shown in Figure 2. The decrease of the coherence for larger f_* may be caused by the turbulence generated on the slope. The flow on the impermeable slope appeared more chaotic than the flow on the corresponding permeable slope. The decrease of

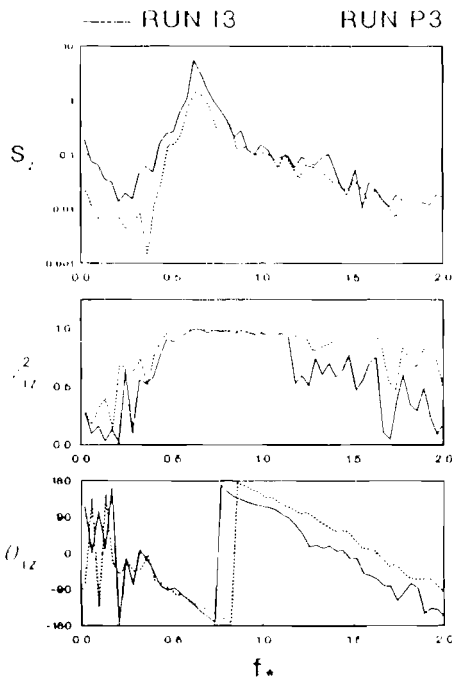


Figure 8. Spectrum, coherence and phase of waterline oscillations for runs I3 and P3.

the coherence for smaller f , suggests that the low frequency wave components in the waterline oscillation on the slope are not strongly correlated to the incident low frequency wave components and may be generated partly by the nonlinear wave interactions on the slope. For the frequency range of the high coherence, the phase difference θ_{12} is related to the normalized travel time given by $-\theta_{12}/(2\pi f_*)$ for the wave component with given f_* propagating from the toe of the slope to the moving waterline. The normalized upslope travel time on the impermeable slope is slightly greater than that on the corresponding permeable slope.

The time series $[Z_r(t) - \bar{Z}_r]$ of the six test runs are also analyzed using a zero upcrossing method. The maximum value of $Z_r(t)$ between the two adjacent zero upcrossings in the time series $[Z_r(t) - \bar{Z}_r]$ is denoted by R_j with $j = 1, 2, \dots, N_o$ where $(N_o + 1)$ is the number of the zero upcrossings. The individual runup heights R_j above SWL are ranked in the descending order. The maximum runup, R_{max} , is the runup height corresponding to the first rank. The sig-

nificant runup R_s is defined as the average of the highest one-third runup heights. On the other hand, the swash height is defined as the difference between the maximum and minimum values of $Z_r(t)$ between the two adjacent zero upcrossings. The significant swash height, h_s , is defined as the average of the highest one-third swash heights. It should be noted that the minimum values of Z_r are sensitive to the elevation of the waterline meter above the rough surface since a thin layer of water remains on the slope during the wave downrush. Table 2 lists the values of h_s/H_s , R_s/H_s , and R_{max}/H_s for the six test runs. These parameters increase with the increase of the surf similarity parameter ξ . The reduction of the wave runup and swash heights caused by the permeability effects is more pronounced for larger values of ξ . These trends are similar to the results for regular wave runup and run-down presented by LOSADA and GIMENEZ-CURTO (1981). The empirical formula for the maximum runup R_{max} proposed by AHRENS and HEIMBAUGH (1988) was found to fall between the values of R_{max} for the corresponding impermeable and permeable slope test runs (COX, 1989). This is probably because the riprap revetments tested by them were permeable but not as permeable as the thick gravel layer used in this experiment.

In order to calculate the runup distribution for each run, the exceedance probability P corresponding to the runup height R_p of the n -th rank is estimated by $P = n/(N_o + 1)$. If the probability distribution of runup heights follows the Rayleigh distribution (BATTJES, 1971; LOSADA and GIMENEZ-CURTO, 1981), the exceedance probability P associated with R_p is given by $P = \exp[-2(R_p/R_s)^2]$. The Rayleigh distribution yields $P = 1$ for $R_p = 0$ and does not account for the wave setup \bar{Z}_r , whereas the definition of the runup height adopted herein results in $R_p > \bar{Z}_r$. As a result, the Rayleigh distribution may not fit the runup distribution in the vicinity of $P = 1$ if the wave setup is not negligible.

Figure 9 shows the exceedance probability P as a function of R_p/R_s together with the Rayleigh distribution for the six test runs. This figure is intended to examine the residual effects of the slope permeability on the normalized runup R_p/R_s , where the significant runup R_s listed in Table 2 already includes the permeability effects. The data points for the six test

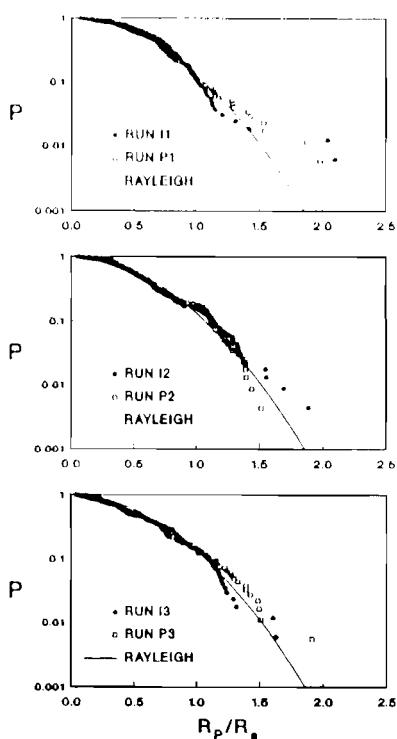


Figure 9. Exceedance probability of normalized runup as compared with Rayleigh distribution for six test runs.

runs follow the Rayleigh distribution fairly well in the range of P greater than approximately 0.02. In this range of P , most of the permeability effects appear to be accounted for by the different values of R_s for the impermeable and permeable slopes. In the range of very small exceedance probability, the Rayleigh distribution does not represent the data points well. Comparing the measured time series $\eta_i(t)$ and $Z_i(t)$ for each run, the runup distribution in the range of very small exceedance probability appears to be affected by the sequence of incident waves and their interaction on the impermeable or permeable slope. Consequently, any simple runup distribution will not fit the data points in this range of P . It should be noted that the present comparison is deterministic since the number of test runs is six and limited. The Rayleigh distribution might represent a large number of data points on an average even in the range of P less than approximately 0.02.

CONCLUSIONS

Irregular wave reflection and runup on rough impermeable and permeable slopes were examined on the basis of the spectral and time series analyses of the measurements for six test runs performed in a wave tank. The permeability effects were found to reduce wave reflection and runup as was observed by a number of researchers. The permeability effects on irregular wave reflection reduced the reflection coefficient fairly uniformly over the wind wave frequency range. The wave reflection from the permeable slope was inferred to occur mainly at the surface of the permeable layer. However, existing spectral methods may not be sufficient for the quantitative interpretations of the highly nonlinear wave processes on the 1:3 slopes. The permeability effects on irregular wave runup were found to reduce the low frequency wave components significantly without affecting the high frequency wave components appreciably. The low frequency wave components in the waterline oscillation on the slope were not strongly correlated to the incident low frequency wave components. This suggests that these low frequency wave components may be generated partly by the nonlinear wave interactions on the slope. Furthermore, the permeability effects were found to reduce wave setup, significant swash height, significant runup and maximum runup significantly. The measured runup distributions in the range of the exceedance probability greater than approximately 0.02 were represented by the Rayleigh distribution fairly well. More extensive data with a better reproduction of incident irregular waves including group bounded long waves will be required to investigate extreme runup heights deterministically and probabilistically.

ACKNOWLEDGEMENTS

This work is a result of research sponsored by the National Science Foundation under grant CTS-8900640 and NOAA Office of Sea Grant, Department of Commerce under grant NA85AA-D-SG033 (SG89 R/OE-5).

LITERATURE CITED

AHRENS, J.P., 1983. Wave runup on idealized structures. *Proceedings of Coastal Structures '83*, American Society of Civil Engineers, pp. 925-938.

- AHRENS, J.P. and HEIMBAUGH, M.S., 1988. Irregular wave runup on riprap revetments. *Journal of Waterway, Port, Coastal and Ocean Engineering*, American Society of Civil Engineers, 114(4), 524–530.
- BARTHEL, V.; MANSARD, E.P.D.; SAND, S.E., and VIS, F.C., 1983. Group bounded long waves in physical models. *Ocean Engineering*, 10(4), 261–294.
- BATTJES, J.A., 1971. Runup distributions of waves breaking on slopes. *Journal of Waterways, Harbors and Coastal Engineering Division*, American Society of Civil Engineers, 97(1), 91–114.
- BOUWS, E.; GUNTHER, H.; ROSENTHAL, W., and VINCENT, C.L., 1985. Similarity of wind wave spectrum in finite depth water. 1. Spectral form. *Journal of Geophysical Research*, 90(C1), 975–986.
- BRUUN, P. and JOHANNESSEN, P., 1976. Parameters affecting stability of rubble mounds. *Journal of Waterway, Harbors and Coastal Engineering Division*, American Society of Civil Engineers, 102(2), 141–164.
- BRUUN, P., Ed., 1985. *Design and Construction of Mounds for Breakwaters and Coastal Protection*. New York: Elsevier, 938p.
- COX, D.T., 1989. Irregular wave reflection and runup on rough, permeable slopes. Thesis for Master of Civil Engineering presented to the University of Delaware, Newark, Delaware, 214p.
- ELGAR, S.; GUZA, R.T., and SEYMOUR, R.J., 1984. Groups of waves in shallow water. *Journal of Geophysical Research*, 89(C3), 3623–3634.
- GODA, Y., 1985. *Random Seas and Design of Maritime Structures*. Tokyo: University of Tokyo Press, 323p.
- GUZA, R.T. and THORNTON, E.B., 1982. Swash oscillations on a natural beach. *Journal of Geophysical Research*, 87(C1), 483–491.
- HOLMAN, R.A. and SALLENGER, A.H., 1985. Setup and swash on a natural beach. *Journal of Geophysical Research*, 90(C1), 945–953.
- KOSTENSE, J.K., 1984. Measurements of surf beat and set-down beneath wave groups. *Proceedings of 19th Coastal Engineering Conference*, American Society of Civil Engineers, pp. 724–740.
- LONGUET-HIGGINS, M.S. and STEWART, R.W., 1962. Radiation stress and mass transport in gravity waves, with application to 'surf beat'. *Journal of Fluid Mechanics*, 13, 481–504.
- LOSADA, M.A. and GIMENEZ-CURTO, L.A., 1981. Flow characteristics on rough, permeable slopes under wave action. *Coastal Engineering*, 4(3), 187–206.
- MADSEN, O.S., 1971. On the generation of long waves. *Journal of Geophysical Research*, 76(36), 8672–8683.
- MANSARD, E.P.D. and BARTHEL, V., 1984. Shoaling properties of bounded long waves. *Proceedings of 19th Coastal Engineering Conference*, American Society of Civil Engineers, pp. 798–814.
- MILGRAM, J.H., 1970. Active water-wave absorbers. *Journal of Fluid Mechanics*, 42(4), 845–859.
- SEELIG, W.N., 1980. Two-dimensional tests of wave transmission and reflection characteristics of laboratory breakwaters. *Technical Report No. 80-1*, U.S. Army Coastal Engineering Research Center, Fort Belvoir, Virginia, 187p.
- SEELIG, W.N., 1983. Wave reflection from coastal structures. *Proceedings of Coastal Structures '83*, American Society of Civil Engineers, pp. 961–973.
- TATAVARTI, R.V.S.N.; HUNTLEY, D.A., and BOWEN, A.J., 1988. Incoming and outgoing wave interactions on beaches. *Proceedings of 21st Coastal Engineering Conference*, American Society of Civil Engineers, pp. 136–150.
- THORNTON, E.B. and CALHOUN, R.J., 1972. Spectral resolution of breakwater reflected waves. *Journal of Waterway, Harbor, Coastal Engineering Division*, American Society of Civil Engineers, 98(4), 443–460.
- VAN DER MEER, J.W., 1988. Deterministic and probabilistic design of breakwater armor layers. *Journal of Waterway, Port, Coastal and Ocean Engineering*, American Society of Civil Engineers, 114(1), 66–80.

□ RÉSUMÉ □

On a élaboré six tests à petite échelle pour examiner le détail des caractéristiques spectrales et des séries temporelles de la réflexion d'une houle irrégulière et son amplification sur des pentes rugueuses de 1/3, perméables et imperméables. La perméabilité réduit le coefficient de réflexion et une amplification significative a été observée par de nombreux chercheurs. Les effets de la perméabilité sur la réflexion des houles irrégulières réduit le coefficient de réflexion à peu près uniformément pendant l'intervalle de fréquence de la mer du vent. Les effets de la perméabilité sur l'amplification de la houle réduisent significativement les composantes de basses fréquences de la houle. L'amplification mesurée dans l'intervalle où la probabilité d'excès est supérieure à environ 0.02 est bien représentée par une distribution de Raleigh.—Catherine Bressolier-Bousquet, Géomorphologie, EPHE, Mont-rouge, France.